Applications of Mathematics

Petr Salač

Numerical solution of the pressing devices shape optimization problem in the glass industry

Applications of Mathematics, Vol. 63 (2018), No. 6, 643–664

Persistent URL: http://dml.cz/dmlcz/147562

63 (2018) APPLICATIONS OF MATHEMATICS No. 6, 643–664

NUMERICAL SOLUTION OF THE PRESSING DEVICES SHAPE OPTIMIZATION PROBLEM IN THE GLASS INDUSTRY

Petr Salač, Liberec

Received September 19, 2017. Published online November 16, 2018.

Abstract. In this contribution, we present the problem of shape optimization of the plunger cooling which comes from the forming process in the glass industry. We look for a shape of the inner surface of the insulation barrier located in the plunger cavity so as to achieve a constant predetermined temperature on the outward surface of the plunger. A rotationally symmetric system, composed of the mould, the glass piece, the plunger, the insulation barrier and the plunger cavity, is considered. The state problem is given as a multiphysics problem where solidifying molten glass is cooled from the inside by water flowing through the plunger cavity and from the outside by the environment surrounding the mould.

The cost functional is defined as the squared L^2_r norm of the difference between a prescribed constant and the temperature on the outward boundary of the plunger. The temperature distribution is controlled by changing the insulation barrier wall thickness.

The numerical results of the optimization to the required target temperature 800 °C of the outward plunger surface together with the distribution of temperatures along the interface between the plunger and the glass piece before, during and after the optimization process are presented.

Keywords: shape optimization; heat-conducting fluid; energy transfer

MSC 2010: 49Q10, 76D55, 93C20

1. Introduction

There are several possibilities for increasing the quality of the surface of glass products and, moreover, to shorten the time needed to press one piece. Imagine the pressing process of a big glass vase: At the beginning, a drop of hot glass falls down into the mould, then the plunger comes down to press the vase and stays about

This work was realized with financial support of the Technological Agency of the Czech Republic, project No. TA03010852.

13 seconds in the down position. Then the plunger leaves the vase. This is the critical moment of the pressing process. If the surface of the plunger is too hot in any place at the moment of separation, the glass melt adheres to the device and the moulded piece deforms. On the other hand, if the surface of the plunger is too cold, small fire cracks appear on the surface of the moulded piece. These two instances both mean poorer quality of production. For these reasons, it is necessary to achieve a given constant distribution of temperature along the surface of the plunger at the moment of separation. We can control this by changing the shape of the cooling cavity, the local speed of the cooling medium, the heat properties of the cooling medium and the heat conductivity of the plunger material. One of the most effective ways to control the distribution of the temperature along the outward surface of the plunger is to change the shape of the inner cooling cavity located at the axis of the plunger. The actual thermal conductivity of the plunger material is too high for good results to be achieved. For this reason, we apply a so-called insulation barrier with significantly lower thermal conductivity located inside the given plunger cavity, thusly enhancing this effect. The plunger is cooled by permanently flowing water which comes into the deepest part of the cavity by a filling tube located in the axis of the plunger; and on its way back, it cools the plunger from the inside. The original construction of the cavity was made by drilling holes of different radii and depths. This construction causes whirls in the flowing water which play negative roles. The new construction eliminates whirls by the smooth surface of the cavity.

2. Formulation of the problem

First we describe the geometry of the whole system in which the pressing takes place. The system consists of the mould, the glass piece, the plunger, the insulation barrier and the plunger cavity. We turn the system to the horizontal position to be able to describe the optimized insulation barrier surface by a function of one variable.

We define the set of admissible functions as

$$U_{\mathrm{ad}}^e = \left\{ F_4^e \in C^{(0),1}([x_P, x_H]);\ F_4^e(x) = \begin{cases} 0 & \text{for } x \in [x_P, x_B^e], \\ f_4^e(x) & \text{for } x \in [x_B^e, x_H], \end{cases} \right.$$
$$x_B^e \in]x_P, x_T - s_{\min}],\ x_P < x_T - s_{\min} < x_H \text{ given constants},$$
$$f_4^e \in C^{(0),1}([x_B^e, x_H]),\ f_4^e(x_B^e) = 0,\ f_3(x) + s_{\min} \leqslant f_4^e(x) \leqslant f_2(x),$$
$$f_2 \in C([x_P, x_H]),\ f_2(x_P) = 0 \text{ given},$$
$$f_3(x) = \left\{ \begin{cases} 0 & \text{for } x \in [x_B^e, x_T - s_{\min}[, \\ a & \text{for } x \in [x_T - s_{\min}, x_H], \end{cases} \quad a > 0,\ s_{\min} > 0 \right\},$$

where f_2, f_3 are fixed functions and $s_{\min} > 0$ is a fixed constant given by the minimal thickness of the gap between the inner plunger wall and the filling tube with radius $a > 0$. The function f_4^e represents the shape of the insulation barrier located in the plunger cavity.

We assume the region Ω_{Ba}^e that depends on the design function F_4^e and that is defined by the formula

$$\Omega_{\mathrm{Ba}}^e = \{(x,r) \in R^2;\ F_4^e(x) < r < f_2(x) \quad \text{for } x \in [x_P, x_H]\}.$$

Denote by Θ the set of all admissible regions $\Omega_{\mathrm{Ba}}^e \subset R^2$, i.e. regions characterized by $F_4^e \in U_{\mathrm{ad}}^e$. Let us define the convergence on the set Θ. Since each Ω_{Ba}^e is uniquely related to F_4^e, we can say that, for $n \to \infty$, a sequence $\Omega_{\mathrm{Ba}}^n \in \Theta$ converges to a region $\Omega_{\mathrm{Ba}}^e \in \Theta$ if and only if the sequence of functions ${}^nF_4^e$ converges uniformly in $[x_P, x_H]$ to the function F_4^e that defines Ω_{Ba}^e.

We consider the planar region $\Omega = \mathrm{Int}\,\overline{\Omega_{\mathrm{Mo}} \cup \Omega_{\mathrm{Gl}} \cup \Omega_{\mathrm{Pl}} \cup \Omega_{\mathrm{Ba}}^e \cup \Omega_{\mathrm{Ca}}^e}$ that represents the planar cross section of the mould, the glass piece, the plunger, the insulation barrier and the cooling channel of the plunger (see Figure 1).

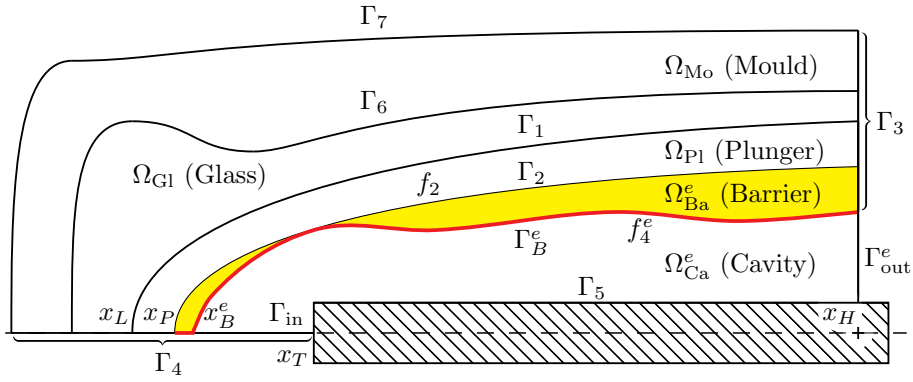

Figure 1. Scheme of the complete system with optimized part of boundary.

Furthermore, we denote by Γ_1 the boundary between the plunger Ω_{Pl} and the moulded piece Ω_{Gl}, Γ_2 the boundary between the plunger Ω_{Pl} and the insulation barrier Ω_{Ba}^e and Γ_B^e the boundary between the insulation barrier Ω_{Ba}^e and the plunger cavity Ω_{Ca}^e. We denote by Γ_3 the part of the boundary connecting the mould, the moulded piece, the plunger and the insulation barrier with the presser, by Γ_4 a part of the axis of symmetry (see Figure 1), by Γ_5 the part of the boundary formed by the tube. Moreover, Γ_6 is the notation for the part of the boundary between the moulded piece Ω_{Gl} and the mould Ω_{Mo} and Γ_7 is the outward boundary of the mould, which is surrounded by an external environment. Furthermore, Γ_{in} denotes the part of the

boundary, where the cooling water comes into the cooling channel of the plunger, and $\Gamma^e_{\rm out}$ stands for the part of the boundary, where the water exits the channel.

We introduce the weighted Sobolev space $H^1_r(\Omega_i)$ (see [2]) provided with the norm

$$\|v\|_{1,r,\Omega_i} = \left(\int_{\Omega_i} \Big[\Big(\frac{\partial v}{\partial x}\Big)^2 + \Big(\frac{\partial v}{\partial r}\Big)^2 + v^2\Big] r \,\mathrm{d}\Omega\right)^{1/2}, \quad i = 0,1,2,3,4, \tag{2.1}$$

($\Omega_0 \equiv \Omega_{\rm Pl}$, $\Omega_1 \equiv \Omega_{\rm Gl}$, $\Omega_2 \equiv \Omega^e_{\rm Ca}$, $\Omega_3 \equiv \Omega_{\rm Mo}$, $\Omega_4 \equiv \Omega^e_{\rm Ba}$).

2.1. Water flow in the plunger cavity. We consider an incompressible potential flow of water, which is rotationally symmetric with respect to the x-axis.

The potential Φ is given as a solution of the Neumann problem

$$\begin{aligned} -\frac{\partial^2\Phi}{\partial r^2} - \frac{1}{r}\frac{\partial\Phi}{\partial r} - \frac{\partial^2\Phi}{\partial x^2} &= 0 && \text{in } \Omega^e_{\rm Ca}, \\ \frac{\partial\Phi}{\partial n} &= 0 && \text{on } \Gamma^e_B \cup \Gamma^C_4 \cup \Gamma_5, \\ \frac{\partial\Phi}{\partial n} &= h^{\rm in}_{\rm velo} && \text{on } \Gamma_{\rm in}, \\ \frac{\partial\Phi}{\partial n} &= h^{\rm out}_{\rm velo} && \text{on } \Gamma^e_{\rm out}, \end{aligned} \tag{P$_f$}$$

where $\partial/\partial n$ denotes the derivative with respect to the outward unit normal with respect to the region $\Omega^e_{\rm Ca}$, $\Gamma^C_4 = \{[x;0];\ x \in [x^e_B, x_T]\}$ is the part of boundary $\Omega^e_{\rm Ca}$, $h^{\rm in}_{\rm velo}$ is the normal component of velocity at the entrance $\Gamma_{\rm in}$ ($h^{\rm in}_{\rm velo} < 0$) and $h^{\rm out}_{\rm velo}$ is the normal component of velocity at the exit $\Gamma^e_{\rm out}$. Further, we assume

$$\int_{\Gamma_{\rm in}} h^{\rm in}_{\rm velo} r \,\mathrm{d}\Gamma + \int_{\Gamma^e_{\rm out}} h^{\rm out}_{\rm velo} r \,\mathrm{d}\Gamma = 0. \tag{2.2}$$

The variational formulation for the potential flow is of the following form:

We look for a function $\Phi \in H^1_r(\Omega^e_{\rm Ca})$ such that

$$\begin{aligned} &\int_{\Omega^e_{\rm Ca}} \Big(\frac{\partial\Phi}{\partial x}\frac{\partial\varphi}{\partial x} + \frac{\partial\Phi}{\partial r}\frac{\partial\varphi}{\partial r}\Big) r \,\mathrm{d}\Omega \\ &\qquad = \int_{\Gamma_{\rm in}} h^{\rm in}_{\rm velo}\varphi r \,\mathrm{d}\Gamma + \int_{\Gamma^e_{\rm out}} h^{\rm out}_{\rm velo}\varphi r \,\mathrm{d}\Gamma \quad \forall\,\varphi \in H^1_r(\Omega^e_{\rm Ca}). \end{aligned} \tag{2.3}$$

The velocity field of the flowing water $\boldsymbol{w} = (w_1, w_2)$ in the cavity $\Omega^e_{\rm Ca}$ is given as

$$\boldsymbol{w} = \operatorname{grad}\Phi. \tag{2.4}$$

Theorem 2.1 (Existence and uniqueness of the velocity field)**.** *Under assumption* (2.2) *there exists a unique velocity field of the form* (2.4) *satisfying the estimate of the Euclidean norm in the form*

$$|||\boldsymbol{w}|||_{L^2_r(\Omega^e_{\mathrm{Ca}})} \leqslant c(\|h^{\mathrm{in}}_{\mathrm{velo}}\|_{L^2_r(\Gamma_{\mathrm{in}})} + \|h^{\mathrm{out}}_{\mathrm{velo}}\|_{L^2_r(\Gamma^e_{\mathrm{out}})}). \tag{2.5}$$

P r o o f. See [4], p. 409. □

R e m a r k 2.1. The potential flow pattern in the plunger cavity does not correspond to physical reality, but serves only to determine the direction of energy removal from the cavity.

2.2. Heat source identification. Pressing glass products on a carousel press is a periodic process in which a certain amount of heat energy is drawn from the glass piece during each cycle. The purpose of the heat source identification problem is to simplify the optimization problem. The non-stationary periodic heat flow effect is approximated by the stationary "average flow" caused by the stationary source, which releases the same amount of heat energy in the individual parts of the glass piece during the pressing cycle.

In the first step we have to determine how much heat energy is necessary to be dissipated from different parts of the glass piece Ω_{Gl} (see Figure 1) during one cycle to achieve given constant temperature T_{Γ_1} of the boundary Γ_1 at the moment of the plunger separation t_P.

Problem A. We solve the mixed problem for heat conduction without internal sources for an unknown temperature ϑ_A, which has in cylindrical coordinates the differential form

$$\begin{aligned}
(\mathrm{P}_A)\qquad c_1\varrho_1\frac{\partial\vartheta_A}{\partial t} &= k_1\left(\frac{\partial^2\vartheta_A}{\partial r^2}+\frac{1}{r}\frac{\partial\vartheta_A}{\partial r}+\frac{\partial^2\vartheta_A}{\partial x^2}\right) && \text{in } [0;t_P]\times\Omega_{\mathrm{Gl}},\\
\vartheta_A(0,x,r) &= T_0 && \text{in } \Omega_{\mathrm{Gl}},\\
\vartheta_A(t,x,r) &= T_0-\frac{T_0-T_{\Gamma_1}}{t_P}t && \text{on } [0;t_P]\times\Gamma_1,\\
\vartheta_A(t,x,r) &= T_0-\frac{T_0-T_{\Gamma_1}}{t_M}t && \text{on } [0;t_P]\times\Gamma_6,\\
\frac{\partial\vartheta_A}{\partial n}(t,x,r) &= 0 && \text{on } [0;t_P]\times(\Gamma_3\cup\Gamma_4^G),
\end{aligned}$$

where c_1 is the specific heat of glass, k_1 the coefficient of thermal conductivity of glass, ϱ_1 the density of glass, T_0 the initial glass temperature, T_{Γ_1} the given target temperature on the boundary Γ_1, t_M the moment of the mould and the glass piece separation, $(t_M > t_P)$ and $\Gamma_4^G \subset \Gamma_4$ is the part of boundary Ω_{Gl}.

The problem (P_A) is solved by the Rothe method of time discretization with time step τ for inhomogeneous initial and boundary conditions of the form

$$
\begin{aligned}
(\mathrm{P}_A^k) \quad c_1\varrho_1\vartheta_A^k - k_1\tau\left(\frac{\partial^2\vartheta_A^k}{\partial r^2} + \frac{1}{r}\frac{\partial\vartheta_A^k}{\partial r} + \frac{\partial^2\vartheta_A^k}{\partial x^2}\right) &= c_1\varrho_1\vartheta_A^{k-1} && \text{in } \Omega_{\mathrm{Gl}},\\
\vartheta_A^0(x,r) &= T_0 && \text{in } \Omega_{\mathrm{Gl}},\\
\vartheta_A^k(x,r) &= T_0 - \tau\frac{T_0 - T_{\Gamma_1}}{t_P}k && \text{on } \Gamma_1,\\
\vartheta_A^k(x,r) &= T_0 - \tau\frac{T_0 - T_{\Gamma_1}}{t_M}k && \text{on } \Gamma_6,\\
\frac{\partial\vartheta_A^k}{\partial n}(x,r) &= 0 && \text{on } (\Gamma_3 \cup \Gamma_4^G),
\end{aligned}
$$

for $k = 1, 2, \ldots, N_A$, where $N_A = t_P/\tau$, ϑ_A^k is the approximation of the temperature ϑ_A on the kth time layer.

The goal is to find a stationary problem to the problem (P_A) with a time-independent heat source that would release the same amount of heat energy in one moulding cycle.

Problem B. We are looking for density of heat sources $f(x,r)$ [$\mathrm{W{\cdot}kg^{-1}}$] such that the solution of the stationary heat problem

$$
\begin{aligned}
(\mathrm{P}_B) \quad -k_1\Big(\frac{\partial^2\vartheta_B}{\partial r^2} + \frac{1}{r}\frac{\partial\vartheta_B}{\partial r} + \frac{\partial^2\vartheta_B}{\partial x^2}\Big) &= \varrho_1 f && \text{in } \Omega_{\mathrm{Gl}},\\
\vartheta_B(x,r) &= T_{\Gamma_1} && \text{on } \Gamma_1,\\
\vartheta_B(x,r) &= T_0 - \frac{T_0 - T_{\Gamma_1}}{t_M}t_P && \text{on } \Gamma_6,\\
\frac{\partial\vartheta_B}{\partial n}(x,r) &= 0 && \text{on } \Gamma_3 \cup \Gamma_4^G,
\end{aligned}
$$

matches the solution of the problem (P_A) at time t_P [s].

By solving the problem A, we want to find the amount of thermal energy that leads to the way of cooling, which achieves the desired temperature T_{Γ_1} [K] on the surface Γ_1 at the time of separation of the glass piece and the plunger t_P [s], and on the surface Γ_6 at the time of separation of the glass piece and the mould t_M [s]. We are looking for a thermal source f of the hypothetical stationary problem B, which locally releases this amount of energy during the course of time from 0 to t_P in the region Ω_{Gl}.

Denote by $\Omega_{\rm Loc} \subset \Omega_{\rm Gl}$ an arbitrarily small subregion of $\Omega_{\rm Gl}$. Then we can express the local amount of heat energy emitted from $\Omega_{\rm Loc}$ during one plunger cycle as

$$c_1 \varrho_1 \int_0^{t_P}\int_{\Omega_{\rm Loc}} \frac{\partial \vartheta_A}{\partial t}\,\mathrm{d}\Omega\,\mathrm{d}t = k_1 \int_0^{t_P}\int_{\Omega_{\rm Loc}} \Big(\frac{\partial^2 \vartheta_A}{\partial r^2} + \frac{1}{r}\frac{\partial \vartheta_A}{\partial r} + \frac{\partial^2 \vartheta_A}{\partial x^2}\Big)\,\mathrm{d}\Omega\,\mathrm{d}t$$
$$= k_1 \int_0^{t_P}\int_{\Omega_{\rm Loc}} \Big(\frac{\partial^2 \vartheta_B}{\partial r^2} + \frac{1}{r}\frac{\partial \vartheta_B}{\partial r} + \frac{\partial^2 \vartheta_B}{\partial x^2}\Big)\,\mathrm{d}\Omega\,\mathrm{d}t = -\varrho_1 \int_0^{t_P}\int_{\Omega_{\rm Loc}} f\,\mathrm{d}\Omega\,\mathrm{d}t,$$

thus

$$c_1 \int_0^{t_P}\int_{\Omega_{\rm Loc}} \frac{\partial \vartheta_A}{\partial t}\,\mathrm{d}\Omega\,\mathrm{d}t = -\int_0^{t_P}\int_{\Omega_{\rm Loc}} f\,\mathrm{d}\Omega\,\mathrm{d}t. \tag{2.6}$$

By integration over time interval $[0, t_P]$, we get

$$c_1 \int_{\Omega_{\rm Loc}} (\vartheta_A(t_P, x, r) - \vartheta_A(0, x, r))\,\mathrm{d}\Omega = -t_P \int_{\Omega_{\rm Loc}} f(x, r)\,\mathrm{d}\Omega \quad \text{in } \Omega_{\rm Gl}. \tag{2.7}$$

Because of the fact that the region $\Omega_{\rm Loc}$ is arbitrarily small, we obtain

$$f(x, r) = \frac{c_1}{t_P}(\vartheta_A(0, x, r) - \vartheta_A(t_P, x, r)) \text{ in } \Omega_{\rm Gl}. \tag{2.8}$$

We substitute initial condition $\vartheta_A(0, x, r) = T_0$ and $\vartheta_A(t_P, x, r) = \vartheta_A^{N_A}(x, r)$ to get

$$f(x, r) = \frac{c_1}{t_P}(T_0 - \vartheta_A^{N_A}(x, r)) \text{ in } \Omega_{\rm Gl}, \tag{2.9}$$

where $\vartheta_A^{N_A}(x, r)$ is the solution of the problem (P_A^k). The problem (P_A^k) is solved by the finite element method (FEM) on each time layer. This is the way how to find the values of the function $\vartheta_A^{N_A}(x, r)$ in individual mesh nodes. We substitute $\vartheta_A^{N_A}$ to (2.9) to get values of the density heat sources $f(x, r)$ which we substitute into the state problem for the optimal design of the insulation barrier shape which follows.

2.3. State problem. We generalize the state system defined for the system composed of the mould, the glass piece, the plunger and the plunger cavity, presented in [4], by adding the insulation barrier into the cavity.

The state problem based on the energy equation for the stationary flow $\boldsymbol{w} = (w_1, w_2)$ with steady temperature ϑ has the form

$$
\begin{aligned}
(\mathrm{P}_h)\quad \varrho_2 c_2 \operatorname{grad}\vartheta\cdot\boldsymbol{w} - k_i\Big(\frac{\partial^2\vartheta}{\partial r^2} + \frac{1}{r}\frac{\partial\vartheta}{\partial r} + \frac{\partial^2\vartheta}{\partial x^2}\Big) &= \varrho_1 f && \text{in } \Omega,\\
\vartheta &= \vartheta_{\mathrm{in}} && \text{on } \Gamma_{\mathrm{in}},\\
\frac{\partial\vartheta}{\partial n} &= 0 && \text{on } \Gamma_3\cup\Gamma_4\cup\Gamma_5\cup\Gamma^e_{\mathrm{out}},\\
\Big[k_0\frac{\partial\vartheta}{\partial n}\Big]_{|\Omega_{\mathrm{Pl}}} + \Big[k_4\frac{\partial\vartheta}{\partial n}\Big]_{|\Omega^e_{\mathrm{Ba}}} &= 0 && \text{on } \Gamma_2,\\
\vartheta_{|\Omega_{\mathrm{Pl}}} &= \vartheta_{|\Omega^e_{\mathrm{Ba}}} && \text{on } \Gamma_2,\\
\Big[k_4\frac{\partial\vartheta}{\partial n}\Big]_{|\Omega^e_{\mathrm{Ba}}} + \Big[k_2\frac{\partial\vartheta}{\partial n}\Big]_{|\Omega^e_{\mathrm{Ca}}} &= 0 && \text{on } \Gamma^e_B,\\
\vartheta_{|\Omega^e_{\mathrm{Ba}}} &= \vartheta_{|\Omega^e_{\mathrm{Ca}}} && \text{on } \Gamma^e_B,\\
\Big[k_0\frac{\partial\vartheta}{\partial n}\Big]_{|\Omega_{\mathrm{Pl}}} + \Big[k_1\frac{\partial\vartheta}{\partial n}\Big]_{|\Omega_{\mathrm{Gl}}} &= \beta && \text{on } \Gamma_1,\\
\vartheta_{|\Omega_{\mathrm{Pl}}} &= \vartheta_{|\Omega_{\mathrm{Gl}}} && \text{on } \Gamma_1,\\
\Big[k_3\frac{\partial\vartheta}{\partial n}\Big]_{|\Omega_{\mathrm{Mo}}} + \Big[k_1\frac{\partial\vartheta}{\partial n}\Big]_{|\Omega_{\mathrm{Gl}}} &= \beta && \text{on } \Gamma_6,\\
\vartheta_{|\Omega_{\mathrm{Mo}}} &= \vartheta_{|\Omega_{\mathrm{Gl}}} && \text{on } \Gamma_6,\\
\Big[k_3\frac{\partial\vartheta}{\partial n} + \alpha\vartheta\Big]_{|\Omega_{\mathrm{Mo}}} &= \alpha\vartheta_{\mathrm{ext}} && \text{on } \Gamma_7,
\end{aligned}
$$

where $\boldsymbol{w}$ is the stationary velocity of the flowing water obtained as the solution to the problem (P_f) in Ω^e_{Ca} ($\boldsymbol{w} = 0$ in $\Omega^e_{\mathrm{Ba}}\cup\Omega_{\mathrm{Pl}}\cup\Omega_{\mathrm{Gl}}\cup\Omega_{\mathrm{Mo}}$), the material constant k_i represents the coefficient of thermal conductivity in Ω_i ($\Omega_0 \equiv \Omega_{\mathrm{Pl}}$, $\Omega_1 \equiv \Omega_{\mathrm{Gl}}$, $\Omega_2 \equiv \Omega^e_{\mathrm{Ca}}$, $\Omega_3 \equiv \Omega_{\mathrm{Mo}}$, $\Omega_4 \equiv \Omega^e_{\mathrm{Ba}}$) and ϱ_1, ϱ_2 the density of glass, water, respectively, c_2 the specific heat of cooling water in Ω^e_{Ca}, f is the density of heat sources obtained from (2.9) in Ω_{Gl} ($f = 0$ in $\Omega^e_{\mathrm{Ca}}\cup\Omega^e_{\mathrm{Ba}}\cup\Omega_{\mathrm{Pl}}\cup\Omega_{\mathrm{Mo}}$), ϑ_{in} the absolute temperature of the water at the inlet, $\alpha > 0$ the coefficient of heat-transfer, $\beta > 0$ the flux density of the modified mass of the body (see [7], p. 128) and $\vartheta_{\mathrm{ext}} > 0$ the temperature of the environment. Symbol $[\partial\vartheta/\partial n]_{|\Omega_i}$ denotes the derivative with respect to the outward unit normal with respect to the region Ω_i.

Let us express the function ϑ, see (P_h), as the sum of five functions, that is

$$\vartheta = \vartheta_0 + \vartheta_1 + \vartheta_2 + \vartheta_3 + \vartheta_4,$$

where

$$\vartheta_i = \begin{cases} \vartheta|_{\Omega_i} & \text{in } \Omega_i,\\ 0 & \text{in } \Omega\setminus\Omega_i \end{cases} \qquad \text{for } i = 0,1,2,3,4, \tag{2.10}$$

($\Omega_0 \equiv \Omega_{\mathrm{Pl}}$, $\Omega_1 \equiv \Omega_{\mathrm{Gl}}$, $\Omega_2 \equiv \Omega^e_{\mathrm{Ca}}$, $\Omega_3 \equiv \Omega_{\mathrm{Mo}}$, $\Omega_4 \equiv \Omega^e_{\mathrm{Ba}}$).

Further, we denote by $\vartheta_i|_{\Gamma_j}$ the trace of solution ϑ_i on the boundary Γ_j for i, j if Γ_j is a boundary of Ω_i.

Moreover, we introduce

$$\mathbf{H}(\Omega) = \{\vartheta;\ \vartheta \text{ defined in (2.10)},\ \vartheta_i \in H_r^1(\Omega_i) \text{ for any } i = 0,1,2,3,4,$$
$$\vartheta_3|_{\Gamma_6} = \vartheta_1|_{\Gamma_6},\ \vartheta_1|_{\Gamma_1} = \vartheta_0|_{\Gamma_1},\ \vartheta_0|_{\Gamma_2} = \vartheta_4|_{\Gamma_2},\ \vartheta_4|_{\Gamma_B^e} = \vartheta_2|_{\Gamma_B^e}\}.$$

We define the norm in $\mathbf{H}(\Omega)$ as

$$\|\vartheta\|_{\mathbf{H}} = (\|\vartheta_0\|_{1,r,\Omega_0}^2 + \|\vartheta_1\|_{1,r,\Omega_1}^2 + \|\vartheta_2\|_{1,r,\Omega_2}^2 + \|\vartheta_3\|_{1,r,\Omega_3}^2 + \|\vartheta_4\|_{1,r,\Omega_4}^2)^{1/2}. \tag{2.11}$$

The set $\mathbf{H}(\Omega)$ with the norm (2.11) is a Hilbert space.

By virtue of the rotational symmetry of both the state problem and the function ϑ, the state problem can be formulated variationally in two dimensions similarly to [4].

We define the trilinear form, two bilinear forms and two functionals:

$$\text{Energy}_\Omega^{\text{velo}}(\vartheta, \boldsymbol{w}, \psi) = c_2 \varrho_2 \int_{\Omega_{\text{Ca}}^e} \Big(\frac{\partial \vartheta_2}{\partial x} w_1 + \frac{\partial \vartheta_2}{\partial r} w_2\Big) \psi r \,\mathrm{d}\Omega, \tag{2.12}$$

$$\begin{aligned}\text{Energy}_\Omega^{\text{cond}}(\vartheta, \psi) = {} & k_0 \int_{\Omega_{\text{Pl}}} \Big(\frac{\partial \vartheta_0}{\partial x}\frac{\partial \psi}{\partial x} + \frac{\partial \vartheta_0}{\partial r}\frac{\partial \psi}{\partial r}\Big) r \,\mathrm{d}\Omega \\ & + k_1 \int_{\Omega_{\text{Gl}}} \Big(\frac{\partial \vartheta_1}{\partial x}\frac{\partial \psi}{\partial x} + \frac{\partial \vartheta_1}{\partial r}\frac{\partial \psi}{\partial r}\Big) r \,\mathrm{d}\Omega \\ & + k_2 \int_{\Omega_{\text{Ca}}^e} \Big(\frac{\partial \vartheta_2}{\partial x}\frac{\partial \psi}{\partial x} + \frac{\partial \vartheta_2}{\partial r}\frac{\partial \psi}{\partial r}\Big) r \,\mathrm{d}\Omega \\ & + k_3 \int_{\Omega_{\text{Mo}}} \Big(\frac{\partial \vartheta_3}{\partial x}\frac{\partial \psi}{\partial x} + \frac{\partial \vartheta_3}{\partial r}\frac{\partial \psi}{\partial r}\Big) r \,\mathrm{d}\Omega \\ & + k_4 \int_{\Omega_{\text{Ba}}^e} \Big(\frac{\partial \vartheta_4}{\partial x}\frac{\partial \psi}{\partial x} + \frac{\partial \vartheta_4}{\partial r}\frac{\partial \psi}{\partial r}\Big) r \,\mathrm{d}\Omega,\end{aligned} \tag{2.13}$$

$$\text{Environment}_\Omega(\vartheta, \psi) = \int_{\Gamma_7} \alpha \vartheta_3|_{\Gamma_7} \psi r \,\mathrm{d}\Gamma, \tag{2.14}$$

$$\text{Source}_\Omega(\psi) = \varrho_1 \int_{\Omega_{\text{Gl}}} f \psi r \,\mathrm{d}\Omega, \tag{2.15}$$

$$\text{Coeff}_\Omega(\psi) = \int_{\Gamma_1} \beta \psi r \,\mathrm{d}\Gamma + \int_{\Gamma_6} \beta \psi r \,\mathrm{d}\Gamma + \int_{\Gamma_7} \alpha \vartheta_{\text{ext}} \psi r \,\mathrm{d}\Gamma. \tag{2.16}$$

Further, we denote

$$A_\Omega(\vartheta, \boldsymbol{w}, \psi) = \text{Energy}_\Omega^{\text{velo}}(\vartheta, \boldsymbol{w}, \psi) + \text{Energy}_\Omega^{\text{cond}}(\vartheta, \psi) + \text{Environment}_\Omega(\vartheta, \psi)$$

and

$$F_\Omega(\psi) = \text{Source}_\Omega(\psi) + \text{Coeff}_\Omega(\psi).$$

We denote by $\mathbf{H}^*(\Omega)$ the space dual to the space $\mathbf{H}(\Omega)$ with the norm

$$\|\psi\|_{\mathbf{H}^*} = \sup_{\varphi \neq 0} \frac{A_\Omega(\varphi, \boldsymbol{w}, \psi)}{\|\varphi\|_{\mathbf{H}}}.$$

We define the sets

$$\Omega_H = \Omega \cup \Gamma_{\text{in}}$$

and

$${}^e\mathcal{H}^{2D} = \{v \in C^\infty(\Omega_H);\ v|_{\Gamma_{\text{in}}} = 0\}.$$

Let $\mathbf{H}_0(\Omega)$ be the closure of the set ${}^e\mathcal{H}^{2D}$ in $\mathbf{H}(\Omega)$.

We assume the existence of a function $\vartheta_\Gamma^e \in \mathbf{H}(\Omega)$ such that

$$\vartheta_\Gamma^e|_{\Gamma_{\text{in}}} = \vartheta_{\text{in}} \quad \text{on } \Gamma_{\text{in}}. \tag{2.17}$$

We use the variational formulation of the energy equation to formulate:

The State Problem: We look for a function $\vartheta \equiv \vartheta(F_4^e) \in \mathbf{H}(\Omega)$ such that

$$A_\Omega(\vartheta, \boldsymbol{w}, \psi) = F_\Omega(\psi) \quad \forall\, \psi \in\ \mathbf{H}_0(\Omega), \tag{2.18}$$

$$\vartheta - \vartheta_\Gamma^e \in \mathbf{H}_0(\Omega), \tag{2.19}$$

where $F_4^e \in U_{\text{ad}}^e$ and $\boldsymbol{w}$ is the corresponding flow pattern given as the gradient of the solution to (2.3).

Theorem 2.2 (Existence and uniqueness of the solution of the state problem)**.** *The state problem* (2.18), (2.19) *has a unique solution* $\vartheta(F_4^e)$ *for each* $F_4^e \in U_{\text{ad}}^e$ *and the associated flow pattern* $\boldsymbol{w}$ *obtained as the gradient of the unique solution of* (2.3)*. Moreover, there exists a constant* $C > 0$ *such that*

$$\|\vartheta(F_4^e)\|_{\mathbf{H}} \leqslant C\|F_\Omega\|_{\mathbf{H}^*}. \tag{2.20}$$

P r o o f. It is sufficient to verify the assumptions of the Lax-Milgram Theorem (see also [4]). □

2.4. Shape optimization problem. We define the *cost functional* as

$$\mathcal{J}^B(F_4^e) = \int_{\Gamma_1} (\vartheta(F_4^e)|_{\Gamma_1} - T_{\Gamma_1})^2 r \,\mathrm{d}\Gamma, \tag{2.21}$$

where $\vartheta(F_4^e)|_{\Gamma_1}$ is the Γ_1-trace of the solution $\vartheta(F_4^e)$ of the state problem (2.18), (2.19) in the region Ω_{Pl} and T_{Γ_1} is a given constant representing the known optimal temperature of the plunger surface.

We introduce following:

The Shape Optimization Problem for the Insulation Barrier: We look for the *optimal design* $F_{\mathrm{Opt}} \in U_{\mathrm{ad}}^e$ such that

$$\mathcal{J}^B(F_{\mathrm{Opt}}) \leqslant \mathcal{J}^B(F_4^e) \quad \forall\, F_4^e \in U_{\mathrm{ad}}^e. \tag{2.22}$$

Theorem 2.3 (Existence of solution of the shape optimization problem)**.** *The shape optimization problem for the insulation barrier* (2.22) *has at least one solution.*

P r o o f. We refer to Theorem 2.1 in [1], p. 29; see also [4]. □

3. Sensitivity analysis

The goal of the sensitivity analysis is to suggest a way of modifying the inner shape of the plunger cavity formed by the insulation barrier in order to minimize the cost functional (2.21). The state problem describes the cooling of the hot glass in the region Ω_{Gl} by the cooling water in the region Ω_{Ca}^e. This is justifiable for the introduction of the physical assumption that thermal energy is transmitted through the gradient lines of the temperature field in the plunger and the insulation barrier from the boundary Γ_1 to the boundary Γ_B^e (see also [5]). The control of the temperature distribution at the boundary Γ_1 is based on the local change of thermal resistance caused by the change of the insulation barrier thickness. Therefore, we control the temperature at Γ_1 by moving the boundary Γ_B^e.

We denote $\Omega_{PB}^e = \operatorname{Int}\overline{\Omega_{\mathrm{Pl}} \cup \Omega_{\mathrm{Ba}}^e}$. Let $B \in \Gamma_B^e$ be the boundary point of Ω_{PB}^e and U_B be its two-dimensional neighborhood. Let B_L, $B_R \in \Gamma_B^e$ be boundary points of $\overline{U_B}$ and Γ_L, $\Gamma_R \subset \Omega_{PB}^e$ be the gradient lines of the temperature field in the plunger and barrier such that $B_L \in \Gamma_L$ and $B_R \in \Gamma_R$. Let $A_L^* \in \Gamma_L \cap \Gamma_1$, $A_R^* \in \Gamma_R \cap \Gamma_1$ and $\Omega_{\mathrm{Loc}} \subset \Omega_{PB}^e$ be a subregion bounded by Γ_L, Γ_1^{Loc}, Γ_R, Γ_B^{Loc}, where $\Gamma_1^{\mathrm{Loc}} = \Gamma_1 \cap \overline{\Omega_{\mathrm{Loc}}}$, $\Gamma_B^{\mathrm{Loc}} = \Gamma_B^e \cap \overline{\Omega_{\mathrm{Loc}}}$ (see Figure 2).

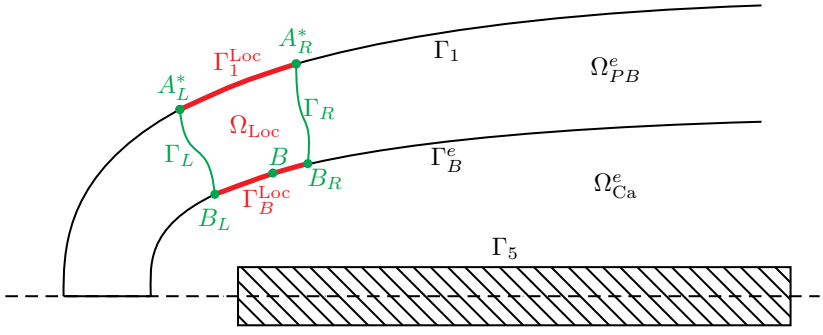

Figure 2. Gradient lines determine the point mapping, which defines the homeomorphism of heat transfer.

We assume the Neumann boundary value problem in Ω_{Loc} as

$$-k_i\Big(\frac{\partial^2\vartheta}{\partial r^2}+\frac{1}{r}\frac{\partial\vartheta}{\partial r}+\frac{\partial^2\vartheta}{\partial x^2}\Big)=0 \quad \text{in } \Omega_{\mathrm{Loc}}, \tag{3.1}$$

$$k_i\frac{\partial\vartheta}{\partial n}=g \quad \text{on } \Gamma_L\cup\Gamma_1^{\mathrm{Loc}}\cup\Gamma_R\cup\Gamma_B^{\mathrm{Loc}}, \tag{3.2}$$

where k_i is the coefficient of thermal conductivity in Ω_i, $i=0,4$, and g some local heat flux.

According to the second law of thermodynamics, we have

$$\frac{\partial\vartheta}{\partial n}=0 \quad \text{on } \Gamma_L\cup\Gamma_R, \tag{3.3}$$

(because Γ_L, Γ_R are the gradient lines of the temperature field), and according to the necessary condition for the existence of the Neumann boundary value problem solution we have

$$k_0\int_{\Gamma_1^{\mathrm{Loc}}}\frac{\partial\vartheta}{\partial n}r\,\mathrm{d}\Gamma=-k_4\int_{\Gamma_B^{\mathrm{Loc}}}\frac{\partial\vartheta}{\partial n}r\,\mathrm{d}\Gamma. \tag{3.4}$$

This equality allows us to define the homeomorphism of heat transfer.

Definition 3.1 (Homeomorphism of heat transfer)**.** The mapping $\mathcal{S}\colon\Gamma_1\to\Gamma_B^e$ is called *the homeomorphism of heat transfer* if: for each segment $\Gamma_1^{\mathrm{Loc}}\subset\Gamma_1$ it holds that the heat energy, which comes into region Ω_{PB}^e through Γ_1^{Loc}, flows away from Ω_{PB}^e through $\mathcal{S}(\Gamma_1^{\mathrm{Loc}})=\Gamma_B^{\mathrm{Loc}}\subset\Gamma_B^e$.

If in some part of Γ_1 we need to decrease the temperature, we locally decrease the heat resistance by moving the points of Γ_B^e along the gradient lines to decrease the thickness of the barrier. On the other hand, in places of Γ_1 where we need higher temperature, we increase thermal resistance by increasing the thickness of the insulation layer, and this will locally decrease the intensity of cooling.

The amount of heat energy that guarantees a decrease of temperature of the surface layer Γ_1^{Loc} of the thickness h from the temperature $\widetilde{\vartheta}_0(A^*)$ (the FEM value of the solution of (3.1), (3.2) at the point $A^*\in\Gamma_1^{\mathrm{Loc}}$, $\mathcal{S}(A^*)=B$) to the temperature T_{Γ_1}, can be approximately expressed in the form

$$Q_{\Gamma_1}^{\mathrm{Loc}}=c_0\varrho_0P_{\Gamma_1}^{\mathrm{Loc}}h(\widetilde{\vartheta}_0(A^*)-T_{\Gamma_1}), \tag{3.5}$$

where $P_{\Gamma_1}^{\mathrm{Loc}}$ is the area created by rotation Γ_1^{Loc} around the x-axis.

This energy must be removed from the subregion Ω_{Loc} through the surface Γ_B^{Loc}, since $\mathcal{S}(\Gamma_1^{\mathrm{Loc}})=\Gamma_B^{\mathrm{Loc}}$. This can be achieved by reducing the temperature $\widetilde{\vartheta}_4(B)$ (the FEM value of the solution of (3.1), (3.2) at the point $B\in\Gamma_B^{\mathrm{Loc}}$) to the value $T_{\Gamma_B^e}$.

The amount of heat energy that causes the temperature $\widetilde{\vartheta}_4(B)$ drop to the desired value $T_{\Gamma^e_B}$ of the surface layer Γ^{Loc}_B of the thickness h can be expressed approximately in the form

$$Q^{\mathrm{Loc}}_{\Gamma_B} = c_4 \varrho_4 P^{\mathrm{Loc}}_{\Gamma_B} h(\widetilde{\vartheta}_4(B) - T_{\Gamma^e_B}), \tag{3.6}$$

where $P^{\mathrm{Loc}}_{\Gamma_B}$ is the area created by rotation Γ^{Loc}_B around the x-axis.

R e m a r k 3.1. Due to the large difference in conductivity between the plunger and the insulation barrier, the insulating resistance of the plunger can be neglected. For this reason we replace the boundary Γ_1 by the boundary Γ_2 in the calculation.

In other considerations, we replace the point A^* with the point A which is the intersection Γ_2 with the temperature gradient line from the point A^*.

We compare (3.5) evaluated on Γ_2 and (3.6) to get

$$c_4 \varrho_4 P^{\mathrm{Loc}}_{\Gamma_2} h(\widetilde{\vartheta}_4(A) - T_{\Gamma_1}) = c_4 \varrho_4 P^{\mathrm{Loc}}_{\Gamma_B} h(\widetilde{\vartheta}_4(B) - T_{\Gamma^e_B}). \tag{3.7}$$

From that we get the estimate for the temperature $T_{\Gamma^e_B}$ associated with T_{Γ_1} as

$$T_{\Gamma^e_B} = \widetilde{\vartheta}_4(B) - \frac{P^{\mathrm{Loc}}_{\Gamma_2}}{P^{\mathrm{Loc}}_{\Gamma_B}} (\widetilde{\vartheta}_4(A) - T_{\Gamma_1}). \tag{3.8}$$

If the thermal gradient line is parallel to the x-axis (e.g. to the axis of the system due to symmetry), problem (3.1) is reduced to the stationary one-dimensional heat conduction in the direction of the x-variable and has a linear solution. If the thermal gradient line is parallel to the r-axis (e.g. in a hypothetical case of a tube shape), problem (3.1) is reduced to the stationary one-dimensional heat conduction for the variable r and has a logarithmic solution. Thus, we can consider that the solution along the gradient line in the general direction has the character between these extreme states. For the purpose of sensitivity analysis, we consider the linear dependence of the temperature on the length of the thermal gradient line.

We consider fixed temperature on the boundary Γ^e_B and replace the gradient line connecting A and B by the straight line connecting A and B (see the analogy for A^i and B^i at Figure 3(a)) to get

$$\frac{T_{\Gamma_1} - \widetilde{\vartheta}_4(B)}{\mathrm{dist}(A,B) - \mathrm{Shift(B)}} = \frac{\widetilde{\vartheta}_4(B) - T_{\Gamma^e_B}}{\mathrm{Shift(B)}}, \tag{3.9}$$

where Shift(B) is the estimate of the point B movement in the direction of vector $\vec{v} = A - B$ that increases or decreases the temperature distribution on Γ^{Loc}_1. From

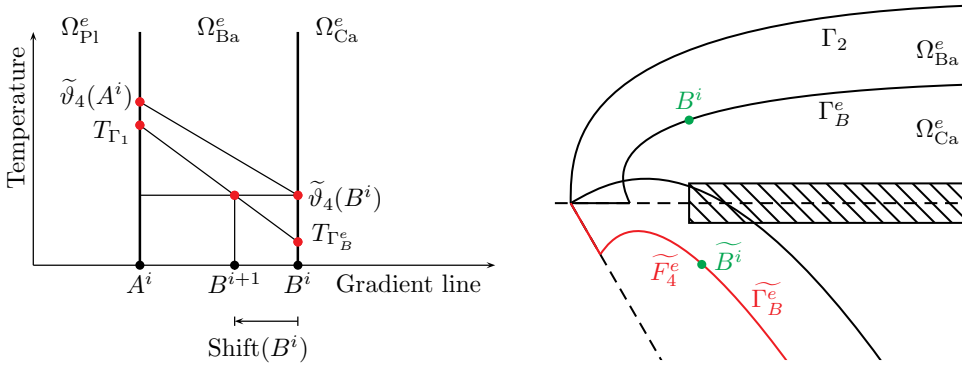

(a) Shift estimate. (b) Scheme of the rotated system.

Figure 3.

that stems

$$\text{Shift(B)} = \operatorname{dist}(A, B)\left(\frac{T_{\Gamma_1} - \widetilde{\vartheta}_4(B)}{\widetilde{\vartheta}_4(B) - T_{\Gamma^e_B}} + 1\right)^{-1}. \tag{3.10}$$

We choose the control points $B^0, B^1, \ldots, B^m \in \Gamma^e_B$ in such a way that

$$B^i = [x_i, f^e_4(x_i)] \quad \text{for } x_P \leqslant x_0 < x_1 < x_2 < \ldots < x_m = x_H$$

and the associated shadow points $A^0, A^1, \ldots, A^m \in \Gamma_2$ such that $B^i = \mathcal{S}(A^i)$ for $i = 0, 1, \ldots, m$.

Further, we denote $A^i = [x_{A^i}, f_2(x_{A^i})]$ for $i = 0, 1, \ldots, m$ and $\Gamma^i_2 \subset \Gamma_2$ is a part of boundary Γ_2 with endpoints A^i_L, A^i_R ($A^i_L \in \Gamma_2$ is the midpoint of $A^{i-1}A^i$ and $A^i_R \in \Gamma_2$ is the midpoint of A^iA^{i+1}), $B^i_L = \mathcal{S}(A^i_L)$ and $B^i_R = \mathcal{S}(A^i_R)$ are images of A^i_L, A^i_R in the homeomorphism of heat transfer.

We approximate

$$P^{\mathrm{Loc}}_{\Gamma_2}(A^i) \approx 2\pi f_2(x_{A^i})\sqrt{(x_{A^i_R} - x_{A^i_L})^2 + (f_2(x_{A^i_R}) - f_2(x_{A^i_L}))^2} \tag{3.11}$$

and

$$P^{\mathrm{Loc}}_{\Gamma_B}(B^i) \approx 2\pi f^e_4(x_i)\sqrt{(x_{B^i_R} - x_{B^i_L})^2 + (f^e_4(x_{B^i_R}) - f^e_4(x_{B^i_L}))^2}. \tag{3.12}$$

We put these approximations into (3.8) and then (3.8) into (3.10) to compute the magnitude of shift of the control point B^i in the direction of vector $\vec{v}^i = A^i - B^i$ for

the next iteration from the formula

$$\text{(3.13)}\quad \operatorname{Shift}(B^i) = \operatorname{dist}(A^i, B^i) \times \left(\frac{f_4^e(x_i)\sqrt{(x_{B_R^i} - x_{B_L^i})^2 + (f_4^e(x_{B_R^i}) - f_4^e(x_{B_L^i}))^2}}{f_2(x_{A^i})\sqrt{(x_{A_R^i} - x_{A_L^i})^2 + (f_2(x_{A_R^i}) - f_2(x_{A_L^i}))^2}} \cdot \frac{T_{\Gamma_1} - \widetilde{\vartheta}_4(B^i)}{\widetilde{\vartheta}_4(A^i) - T_{\Gamma_1}} + 1 \right)^{-1},$$

where $\widetilde{\vartheta}_4$ denotes the solution of state problem (2.18)–(2.19) and T_{Γ_1} the temperature, which the plunger outward surface Γ_1 is optimized on (see Figure 3(a)). Positive value of $\operatorname{Shift}(B^i)$ means shift in the direction of vector $\vec{v}^{\,i}$, i.e. to the region Ω^e_{Ba} (barrier) and negative value of $\operatorname{Shift}(B^i)$ means shift in the direction of vector $-\vec{v}^{\,i}$, i.e. to the region Ω^e_{Ca} (cavity).

The construction of the boundary Γ^e_B is performed in such a way that in each iteration all the control points B^i are first rotated in the negative sense by 60° to the position $\widetilde{B^i}$. In this position, a cubic spline forming a new shape of the boundary $\widetilde{\Gamma^e_B}$ is constructed and this curve is rotated back to the original coordinate system in which other problems are solved. This makes it possible to achieve the shape of the boundary Γ^e_B with negative tangent directive in the lower part of the cavity (see Figure 3(b)).

4. Numerical results

In the numerical experiment, the algorithm for optimization of the insulation barrier for the pressing of the vase made of lead crystal glassware was designed and tuned. The optimized boundary was modelled using the cubic spline. First, the stationary source of heat was found as a heat source identification problem (P^k_A) solution, and then it was used in all algorithm iterations. In each iteration, the components of the potential flow of cooling water were first calculated by solving the problem (P_f), and then the distribution of the temperature throughout the whole system was found by solving the state problem (P_h). Then, the cost functional value for the target temperature $T_{\Gamma_1} = 1073$ [K] (= 800 °C) on Γ_1 was calculated and the new positions of the control points of the optimized inner boundary of the insulation barrier Γ^e_B were determined by the sensitivity analysis. The new insulation barrier boundary shape for the next iteration was designed by passing the cubic spline to the new positions of the control points. Ninety-nine iterations of the process were performed and among them the iteration with the smallest value of the cost functional was found.

4.1. Material properties of the system. We used the parameters of the vase which was measured in laboratory and the results of the experiment were published

in the research report [3]. The vase made from lead crystal glassware of the height $x_H = 0.267$ [m] and of the mass 1.55 kg was pressed in the carousel press where the plunger pressed consecutively in six moulds. The total time of the working cycle was 162 s with the plunger working cycle 27 s.

The molten glass with the density $\varrho_1 = 2500$ [kg/m^3], the specific heat $c_1 = 796$ [J/kg·K] and the coefficient of thermal conductivity $k_1 = 3.8$ [W/m·K] was used in the calculation. The plunger and the mould were made from steel with the density $\varrho_0 = \varrho_3 = 7800$ [kg/m^3], the specific heat $c_0 = c_3 = 482$ [J/kg·K] and the coefficient of thermal conductivity $k_0 = k_3 = 73$ [W/m·K]. The insulation barrier was made from ceramics with the density $\varrho_4 = 4500$ [kg/m^3], the specific heat $c_4 = 900$ [J/kg·K] and the coefficient of thermal conductivity $k_4 = 2.5$ [W/m·K]. The cooling water with the density $\varrho_2 = 1000$ [kg/m^3], the specific heat $c_2 = 4180$ [J/kg·K] and the coefficient of thermal conductivity $k_2 = 0.6$ [W/m·K] was used. The cooling was implemented by the volume $V = 1$[l/min] of water with the temperature $\vartheta_{\text{in}} = 288$ [K] ($= 15\,^\circ$C) at the entrance. The temperature of the environment was $\vartheta_{\text{ext}} = 333$ [K] ($= 60\,^\circ$C). The coefficient of heat-transfer between the mould and the environment was chosen to be $\alpha = 14$ [W/m^2·K] (the value used for underfloor heating). The coefficient of the flux density of the modified mass of body $\beta = 0$. The target temperature of the plunger outward surface Γ_1 was $T_{\Gamma_1} = 1073$ [K] ($= 800\,^\circ$C).

The problem of stationary conduction of heat for mean values of temperatures replaced the real periodical process of cooling.

4.2. Determining the stationary heat source. The stationary heat source was determined as the solution of the heat source identification problem from Section 2.2 with the initial temperature $T_0 = 1423$ [K] ($= 1150\,^\circ$C) in the region Ω_{Gl} and the prescribed linear decrease of temperature to the target temperature $T_{\Gamma_1} = 1073$ [K] ($= 800\,^\circ$C) on the boundary Γ_1 at the time $t_P = 13$ [s] and on the boundary Γ_6 at the time $t_M = 88$ [s].

We solve the problem (P_A) by the method of time discretization as the problem (P_A^k) with time step $\tau = 1$ [s] for inhomogeneous initial and boundary conditions for $k = 1, 2, \ldots, N_A$ with $N_A = 13$. Software FreeFem++ was used. The mesh with 25 781 nodes and 50 511 triangles was generated automatically and the continuous piecewise quadratic Lagrangian elements P2 were used.

The FreeFem++ code for the weak formulation of the time discretized problem (P_A^k) has the form

$$\begin{aligned}\text{problem dHeat}(\vartheta^k, \psi) = \text{int2d}(\Omega_{\text{Gl}})\big((c_1 * \varrho_1 * \vartheta^k * \psi \\ + k_1 * \tau * (\mathrm{d}x(\vartheta^k) * \mathrm{d}x(\psi) + \mathrm{d}y(\vartheta^k) * \mathrm{d}y(\psi))) * y\big)\end{aligned}$$

$$+ \operatorname{int2d}(\Omega_{\mathrm{Gl}})(-c_1 * \varrho_1 * \vartheta^{k-1} * \psi * y)$$
$$+ \operatorname{on}(\Gamma_6, \vartheta^k = g_2) + \operatorname{on}(\Gamma_1, \vartheta^k = g_1),$$

where code variable y represents the (P_A^k) variable r and

$$\vartheta^0(x,r) = T_0 \quad \text{in } \Omega_{\mathrm{Gl}},$$
$$g_1(x,r) = T_0 - \tau \frac{T_0 - T_{\Gamma_1}}{t_P} k \quad \text{on } \Gamma_1,$$
$$g_2(x,r) = T_0 - \tau \frac{T_0 - T_{\Gamma_1}}{t_M} k \quad \text{on } \Gamma_6.$$

We get the stationary heat source in the region Ω_{Gl} in accordance with (2.9). We substitute this numerical solution at the last time layer to the formula

$$f(x,r) = \frac{c_1}{t_P}(T_0 - \vartheta_A^{N_A}(x,r)) \ [\mathrm{W/kg}], \tag{4.1}$$

where $c_1 = 796$ [J/(kg·K)] is the specific heat of glass.

Subsequently, this source was used in all 99 iterations of the optimization problem.

4.3. Determining the velocity of the cooling water. In each iteration of the optimization process we first rotate the eleven points B^i to the points $\widetilde{B^i}$, then construct the boundary $\widetilde{\Gamma_B^e}$ as a natural cubic spline with the eleven control points $\widetilde{B^i}$ and rotate it back to the boundary Γ_B^e. We start with the points

$$[0.015, 0], [0.020, 0.010], [0.030, 0.016], [0.044, 0.018], [0.060, 0.020], [0.085, 0.022],$$
$$[0.118, 0.024], [0.152, 0.025], [0.188, 0.025], [0.226, 0.025], [0.267, 0.025]$$

in the initial iteration.

After we had constructed the plunger cavity Ω_{Ca}^e in the current iteration, we solved the Neumann problem (P_f) to compute the potential of the velocity field of the cooling water. The problem was solved again by FEM using the software FreeFem++. In the initial iteration, the mesh with 853 nodes and 1469 triangles was generated automatically and the continuous piecewise quadratic Lagrangian elements P2 were used.

The FreeFem++ code for the weak formulation of the problem (P_f) has the form

$$\operatorname{problem}\operatorname{Potential}(\Phi, \varphi) = \operatorname{int2d}(\Omega_{\mathrm{Ca}}^e)((\mathrm{d}x(\Phi) * \mathrm{d}x(\varphi) + \mathrm{d}y(\Phi) * \mathrm{d}y(\varphi)) * y)$$
$$- \operatorname{int1d}(\Gamma_{\mathrm{in}})(h_{\mathrm{velo}}^{\mathrm{in}} * \varphi * y) - \operatorname{int1d}(\Gamma_{\mathrm{out}}^e)(h_{\mathrm{velo}}^{\mathrm{out}} * \varphi * y),$$

where

$$h_{\mathrm{velo}}^{\mathrm{in}} = -\frac{V}{\pi * 60 * a^2}, \quad h_{\mathrm{velo}}^{\mathrm{out}} = \frac{V}{\pi * 60 * (y(10)^2 - a^2)},$$

$V = 0.001$ [m^3/min] is the volume of cooling water at the entrance, $a = 0.006$ [m] is the radius of the filling tube and $y(10)$ is the second coordinate of the last control point B^{10}.

We get the velocity field of the flowing water according to (2.4) by putting this numerical solution into the following formulas:

$$w_1 = \begin{cases} \dfrac{\partial \Phi}{\partial x} & \text{in } \Omega^e_{\mathrm{Ca}}, \\ 0 & \text{in } \Omega - \Omega^e_{\mathrm{Ca}}, \end{cases} \tag{4.2}$$

$$w_2 = \begin{cases} \dfrac{\partial \Phi}{\partial r} & \text{in } \Omega^e_{\mathrm{Ca}}, \\ 0 & \text{in } \Omega - \Omega^e_{\mathrm{Ca}}. \end{cases} \tag{4.3}$$

4.4. Determining the distribution of temperature in the system. Both the stationary heat source f from (4.1) and the components of the velocity field of the flowing water w_1, w_2 from (4.2), (4.3) were subsequently substituted into the state problem (P_h).

The problem was solved again by FEM using the software FreeFem++. In the initial iteration, the mesh with 121 586 nodes and 242 425 triangles was generated automatically and the continuous piecewise linear Lagrangian elements P1 were used.

The FreeFem++ code for the state problem (2.18), (2.19) has the form

$$\begin{aligned} \text{problem Thermic}(\vartheta, \psi) = {} & \text{int2d}(\Omega)(((k * (\mathrm{d}x(\vartheta) * \mathrm{d}x(\psi) + \mathrm{d}y(\vartheta) * \mathrm{d}y(\psi))) \\ & + c_2 * \varrho_2 * (w_1 * \mathrm{d}x(\vartheta) * \psi + w_2 * \mathrm{d}y(\vartheta) * \psi)) * y) \\ & - \text{int2d}(\Omega)(\varrho_1 * f * \psi * y) + \text{int1d}(\Gamma_7)(\alpha * \vartheta * \psi * y) \\ & - \text{int1d}(\Gamma_7)(\alpha * \vartheta_{\mathrm{ext}} * \psi * y) + \text{on}(\Gamma_{\mathrm{in}}, \vartheta = \vartheta_{\mathrm{in}}). \end{aligned}$$

R e m a r k 4.1. Numerical computation performed with the actual water conductivity value $k_2 = 0.6\,[\mathrm{W/(m{\cdot}K)}]$, using a potential cooling water flow model in the plunger cavity, shows a completely unrealistic temperature distribution in the direction of the r-axis. In the thin layer at the barrier surface, the water temperature is close to the high barrier temperature and decreases after several millimetres to 18 °C. The cooling water in the rest of the cavity has the temperature approximately 15 °C. This points to the fact that the model of the potential flow of cooling water does not correspond to the physical reality, however, the flow has only an auxiliary character in the plunger cavity, which prefers one direction for the dissipation of heat energy. The introduction of a real model, respecting the change of state of boiling water at the surface of the barrier, would greatly increase the computational difficulty and its effect on the optimization problem would be negligible. The easiest removal of this discrepancy with reality, while maintaining the potential flow model, is a significant

increase in water conductivity, thereby achieving a more natural distribution of temperature in the direction of the r-axis in the plunger cavity. Therefore, we increased the water conductivity ten times and we chose $k_2 = 6$ [W/(m·K)].

4.5. Determining of the new control points' positions. Sensitivity analysis with respect to the temperature along the boundary Γ_1 was implemented in each iteration. We have nine control points $B_j^i \in \Gamma_B^e$ from the previous jth iteration and nine shadow points $A_j^i \in \Gamma_2$ as the intersections of the temperature gradient lines derived from the control points B_j^i. In the shadow points A_j^i we computed the temperatures and compared them with the target temperature required on the outward boundary of the plunger, i.e. $T_{\Gamma_1} = 1073$ [K] $(= 800\,^\circ\mathrm{C})$. If the current temperature in the given shadow point A_j^i was higher than the target temperature, we moved the control point B_j^i in the direction of the temperature gradient to the region Ω_{Ba}^e (barrier); in the opposite case we moved it to the region Ω_{Ca}^e (cavity). The magnitude of this shift was chosen in proportion to the amount of energy we had to take more or less to achieve the target temperature $T_{\Gamma_1} = 1073$ [K]. Analogously, we moved the first control point B_j^0 along the x-axis or the last control point B_j^{10} along the line $x = 0.267$ [m]. The displacement size was chosen according to the assumption of an "almost" linear dependence of the temperature drop on the insulation barrier thickness (see also (3.13)). In each iteration ($(j+1)$th iteration) the new position of the control points B_{j+1}^i was calculated according to the formula

$$B_{j+1}^i = B_j^i + \frac{1}{2}(A_j^i - B_j^i) \times \left(\frac{r_{B_j^i} \cdot \sqrt{(x_{B_{jR}^i} - x_{B_{jL}^i})^2 + (r_{B_{jR}^i} - r_{B_{jL}^i})^2}}{f_2(x_{A_j^i}) \cdot \sqrt{(x_{A_{jR}^i} - x_{A_{jL}^i})^2 + (f_2(x_{A_{jR}^i}) - f_2(x_{A_{jL}^i}))^2}} \cdot \frac{T_{\Gamma_1} - \widetilde{\vartheta}_4(B_j^i)}{\widetilde{\vartheta}_4(A_j^i) - T_{\Gamma_1}} + 1 \right)^{-1}$$
$$i = 0, 1, \ldots, 10,$$

where $\widetilde{\vartheta}_4(A_j^i)$ and $\widetilde{\vartheta}_4(B_j^i)$ denote the solutions of the state problem (2.18)–(2.19) in A_j^i and B_j^i.

The curvilinear integral in the cost functional $\mathcal{J}^B$ was computed numerically with equidistant division into 1000 intervals along the length of the curve representing the boundary Γ_1.

4.6. Results of the iteration process. In the initial iteration the insulation barrier was too thick, causing the value of the cost functional $\mathcal{J}_0^B = 168\,334.33$.

In the subsequent iterations the insulation barrier was significantly thinned, which led to a sharp decline of the cost functional value. In the 10th iteration the value of

the cost functional was $\mathcal{J}_{10}^{B} = 1\,140.44$, the temperature distribution in the system can be seen in Figure 4.

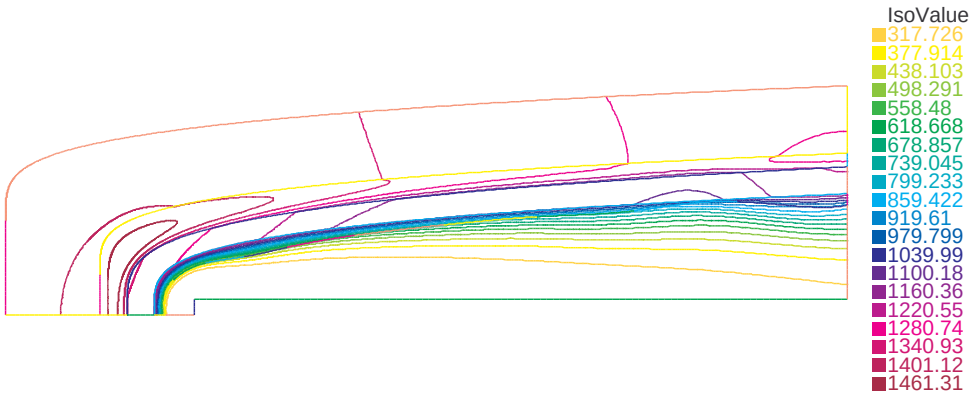

Figure 4. Distribution of temperatures in the 10th iteration.

In the 20th iteration the value of the cost functional was $\mathcal{J}_{20}^{B} = 117.49$, in the 60th iteration the value of the cost functional was $\mathcal{J}_{60}^{B} = 2.992$ and in the last 99th iteration the value of the cost functional was $\mathcal{J}_{99}^{B} = 1.122$. We computed only 99 iterations. The temperature distribution in the system in the 99th iteration is shown in Figure 5.

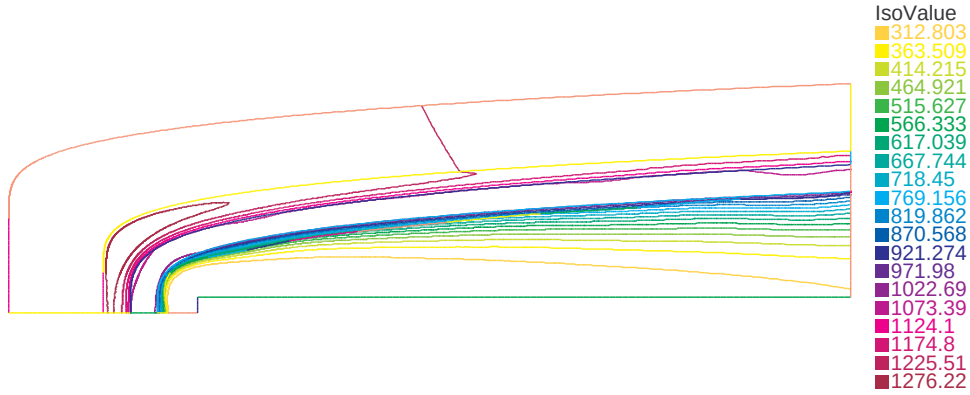

Figure 5. Distribution of temperatures in the 99th iteration.

The following graphs in Figure 6 show the distribution of temperatures measured from the lowest plunger point $[x_L, 0] \in \Gamma_1$ to the point $[x_H, 0.055] \in \Gamma_1$ along the outward plunger surface Γ_1 in the initial iteration, in the 10th, 20th, 60th, 99th iterations and the target temperature $T_{\Gamma_1} = 1073$ [K].

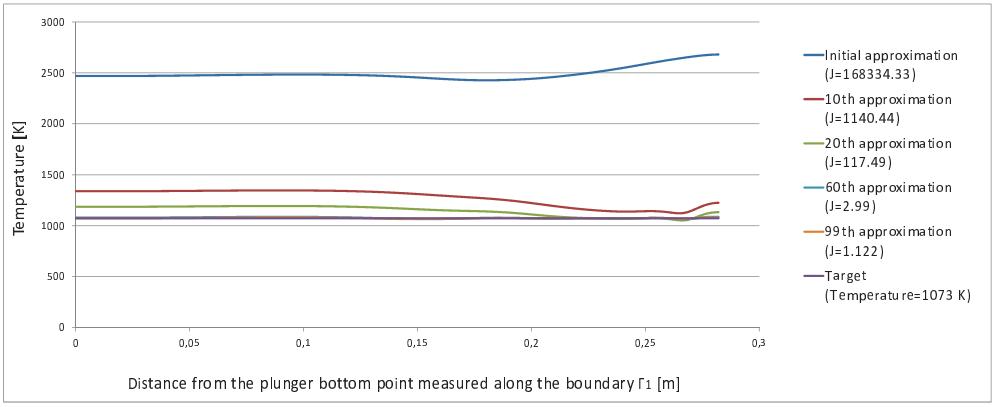

Figure 6. Distribution of temperatures along the outward plunger surface Γ_1.

The graph in Figure 7 has a changed temperature range to highlight the temperature course of the last iterations.

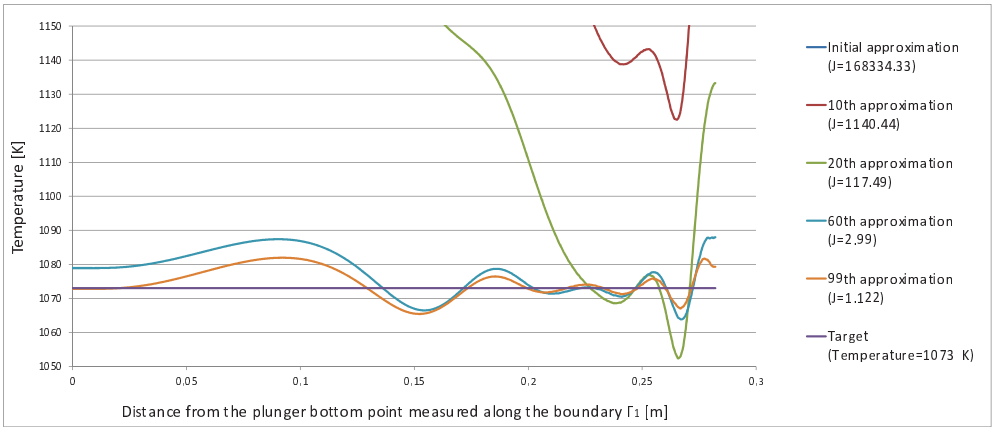

Figure 7. Distribution of temperatures along the outward plunger surface Γ_1 with changed temperature range on the temperature axis.

5. Conclusion

Numerical results show that the proposed algorithm effectively minimizes the value of the cost functional and balances the temperature of the plunger outward surface to the desired value in the considered model.

The laboratory experiment which would verify the degree of compliance of the proposed model for the shape optimization of the insulation barrier with reality, was

not performed. The agreement of the model and reality can only be inferred from an analogy with the similar experimental verification of the model described in [6], in which the optimized shape of the plunger cavity with the application of a regulation current body was considered.

The model should contribute to streamlining the introduction of a new assortment into the production. The original construction of the plunger cavity had been formed by drilling holes of different diameters and depths, where the ceramic rings had been inserted. The design had been based on the observed deficiencies on the surface of the glass pieces from the test series.

References

[1] *J. Haslinger, P. Neittaanmäki*: Finite Element Approximation for Optimal Shape Design: Theory and Applications. John Wiley & Sons, Chichester, 1988. zbl MR

[2] *A. Kufner*: Weighted Sobolev Spaces. A Wiley-Interscience Publication, John Wiley & Sons, New York, 1985. zbl MR

[3] *I. Matoušek, J. Cibulka*: Analýza tvarovacího cyklu na karuselovém lisu NOVA. TU v Liberci, Liberec, 1999. (In Czech.)

[4] *P. Salač*: Optimal design of the cooling plunger cavity. Appl. Math., Praha *58* (2013), 405–422. zbl MR doi

[5] *P. Salač*: Optimization of plunger cavity. Programs and Algorithms of Numerical Mathematics 16, 2012 (J. Chleboun et al., eds.). Academy of Sciences of the Czech Republic, Institute of Mathematics, Praha, 2013, pp. 174–180. zbl MR

[6] *P. Salač, M. Starý*: The cooling of the pressing device in the glass industry. Internat. J. Multiphysics *7* (2013), 207–218. doi

[7] *S. N. Šorin*: Sdílení Tepla. SNTL, Praha, 1968. (In Czech.)

Author's address: *Petr Salač*, Technical University of Liberec, Studentská 2, 461 17 Liberec 1, Czech Republic, e-mail: `petr.salac@tul.cz`.